Electronic and magnetic structure of CsV_2O_5

Roser Valentí[1] and T. Saha-Dasgupta[2]
[1]*Fakultät 7, Theoretische Physik, University of the Saarland, 66041 Saarbrücken, Germany*
[2]*S.N. Bose National Centre for Basic Sciences, JD Block, Sector 3, Salt Lake City, Kolkata 700098, India*
(Received 16 October 2001; published 4 April 2002)

We have studied the electronic structure of the spin-gapped system CsV_2O_5 by means of an *ab initio* calculation. Our analysis and a reexamination of the susceptibility data indicate that the behavior of this system is much closer to that of an alternating spin-$\frac{1}{2}$ antiferromagnetic chain with significant inter-dimer coupling and weaker interchain couplings than that of isolated dimers as was initially proposed. Comparison to the vanadate family members α'-NaV_2O_5, γ-LiV_2O_5, and isostructural compounds like $(VO)_2P_2O_7$ is discussed.

DOI: 10.1103/PhysRevB.65.144445 PACS number(s): 75.30.Gw, 75.10.Jm, 78.30.−j

I. INTRODUCTION

Low-dimensional spin-gapped quantum systems are of current interest since they show interesting ground states and a variety of unconventional low-lying excitations. Examples of such systems include spin-1 Haldane chains,[1] spin-$\frac{1}{2}$ even-leg ladders[2] and spin-$\frac{1}{2}$ alternating chains.[3] The discovery of appropriate compounds like Y_2BaNiO_5 (Ref. 4) (Haldane chain), $Sr_{14}Cu_{24}O_{41}$ (Ref. 5), or $SrCu_2O_3$ (Ref. 6) (ladder systems) has brought new insight into the study of these systems. There is a long list of various spin-$\frac{1}{2}$ alternating chain systems which are being intensively studied in connection to their magnetic excitations, to mention a few of them: $KCuCl_3$,[7] $TlCuCl_3$,[8] and $Cu(NO_3)_2\cdot\frac{5}{2}D_2O$.[9] If frustration is also present, new features appear in the magnetization spectrum of the low-dimensional quantum systems as in $CuGeO_3$,[10] $(VO)_2P_2O_7$ (VOPO),[11] $SrCu_2(BO_3)_2$,[12] or the recently synthesized $Cu_2Te_2O_5Br_2$.[13]

An important family of low-dimensional compounds is composed of the layered vanadates AV_2O_5 (A=Ca, Mg, Na, Li, Cs).[14] While CaV_2O_5 and MgV_2O_5 contain only magnetic V^{4+} ions and behave like spin-$\frac{1}{2}$ ladders with spin gaps of the order of 600 K (Ref. 15) and 20 K (Ref. 16), respectively, α'-NaV_2O_5, γ-LiV_2O_5, and CsV_2O_5 are mixed-valence systems ($V^{4.5+}$ on average) with important charge and spin fluctuations. This last property makes this family especially interesting since it allows us to study the influence of charge ordering and the corresponding crystallographic distortions on the magnetic interactions. The quarter-filled ladder compound α'-NaV_2O_5 (Refs. 17, and 18) is a highly discussed material and has become a model substance for the study of spin, charge, and orbital coupling. It behaves like a spin-$\frac{1}{2}$ Heisenberg system at high temperatures and at 34 K undergoes a charge ordering ($2V^{4.5+}\rightarrow V^{4+}+V^{5+}$) transition[19] accompanied by a lattice distortion[20] and the opening of a spin gap.[21] γ-LiV_2O_5 is a charge-ordered system with no spin-gap opening at low temperatures.[22] Recent investigations based on an *ab initio* analysis of the electronic structure[23] show that charge fluctuations in this system are still significant and the experimental observations[22,24] can be well described by a spin-$\frac{1}{2}$ asymmetric quarter-filled ladder model. Such a proposal has also found support by a numerical analysis of optical conductivity experiments.[25] The third member of this vanadate family, CsV_2O_5, has been given much less attention. The existing susceptibility measurements of Isobe and Ueda[22] could be rather well explained by considering this material as a system of isolated dimers with a spin gap of $\approx$12 meV. Measurements other than that are unknown to us except for older susceptibility measurements[26] which somewhat disagree with Isobe and Ueda's data and different values of the exchange integral J and the gyromagnetic ratio g are predicted.

There are various reasons why we believe that this system deserves attention: (i) The question of how the electronic and magnetic properties of this material compare with the properties of the other two members of the alkali-vanadate family, i.e., α'-NaV_2O_5 and γ-LiV_2O_5. (ii) This system crystallizes in a similar monoclinic structure as the most discussed VOPO and many other materials, e.g., $KCuCl_3$ and $TlCuCl_3$, showing an alternating chain behavior of the magnetic interactions. It is then worthwhile to find out whether CsV_2O_5 has also a similar behavior of the magnetic interactions as its isostructural members. (iii) As will be shown below, a reexamination of the susceptibility measurements reveals that a dimer model is not the only model that can provide a reasonable fitting of the susceptibility data.

In view of the above, we have performed a microscopic study of this system by considering density-functional-theory-based (DFT) calculations. The microscopic study of the electronic behavior of this compound reveals that the interdimer coupling in this material in addition to the intradimer interaction is also significant and should not be neglected. Further, an analysis of the susceptibility data shows that getting estimates of the coupling constants and the gyromagnetic factor based merely on a fitting procedure is very subtle and with such an analysis one can only test the consistency with the assumed model, but cannot prove the uniqueness of that model. Results of that will be presented in the next sections. We shall also discuss the similarities and differences to the other members of this vanadate family, α'-NaV_2O_5, and γ-LiV_2O_5, as well as to isostructural compounds like VOPO.

II. CRYSTAL STRUCTURE

The crystal structure of CsV_2O_5 is somewhat different from that of α'-NaV_2O_5 and γ-LiV_2O_5. α'-NaV_2O_5 and

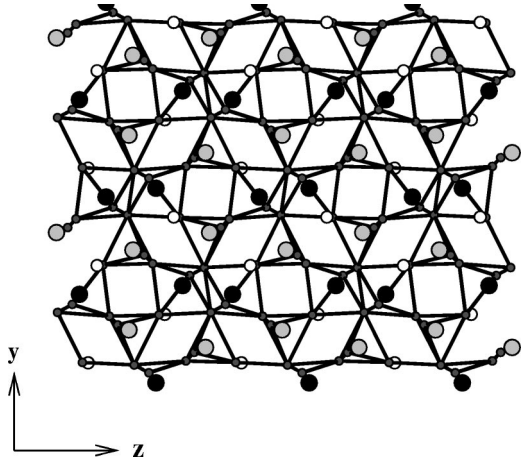

FIG. 1. Crystal structure of CsV_2O_5 projected in the (yz) plane (see text for explanation). The large circles are the V ions, black and grey for V^{4+} and V^{5+}, respectively. The oxygens are represented by the smaller circles. Pairs of edge-shared distorted V^{4+} O_5 square pyramids are bridged by V^{5+} O_4 tetrahedra to form layers. The alkali-ion Cs shown by white circles are located in between these sheets.

γ-LiV_2O_5 crystallize in the orthorhombic space group $Pmmn$ (D_{2h}^{13}) and $Pnma$ (D_{2h}^{16}), respectively. They consist of a double-chain structure of edge-sharing distorted square VO_5 pyramids running along the orthorhombic y axis, which are linked together via common corners to form layers. These layers are stacked upon each other along z. Na/Li atoms are located between these layers. CsV_2O_5 crystallizes,[27] on the other hand, in the monoclinic space group $P2_1/c$ (C_{2h}^5). CsV_2O_5 has also a layered structure with Cs ions in between the layers. These layers, which are somewhat tilted (i.e., not strictly in the yz plane) and are stacked upon each other along x, are made of two types of vanadium atoms V1 and V2. The V1 atoms are in a distorted square pyramidal environment of oxygens and form pairs by sharing the edge of the pyramids. These pairs are separated from one another by the V2 vanadiums in a tetrahedral coordination of oxygens as shown in Fig. 1. Within a pair of square pyramids, the two apical O atoms are pointing in opposite directions and the remaining O atoms of the pyramids are shared with tetrahedra. The V1-V1 distance across the shared edge of the square pyramid pair is 3.073 Å and the V1-V2 distance across the shared corner of a pyramid and a tetrahedron is 3.352 Å. Since the average V2-O distance within the tetrahedron, $d=1.718$ Å, is shorter than the average V1-O distance within the square pyramid, $d=1.882$ Å, one can conclude from a bond-valence analysis[27] that the V1 sites are in the oxidation V^{4+} and the V2 sites are in the oxidation V^{5+}. As the intrapair V^{4+}-V^{4+} distance is 3.073 Å while the interpair distance along the z axis is 5.501 Å, this compound has been assumed to be a system of isolated dimers.

III. BAND STRUCTURE

In order to analyze the electronic behavior of CsV_2O_5, we carried out DFT calculations within the local density approximation (LDA) by employing both the WIEN97 (Ref. 28) code based on the full-potential linearized augmented plane wave (LAPW) method and the Stuttgart TBLMTO-47 code based on the linear-muffin-tin orbital (LMTO) (Ref. 29) method. Both calculations agree well within the allowed error bars of the various different approximations involved in the two different methods. In both approaches we treated the exchange-correlation part by using the generalized gradient approximation.[30]

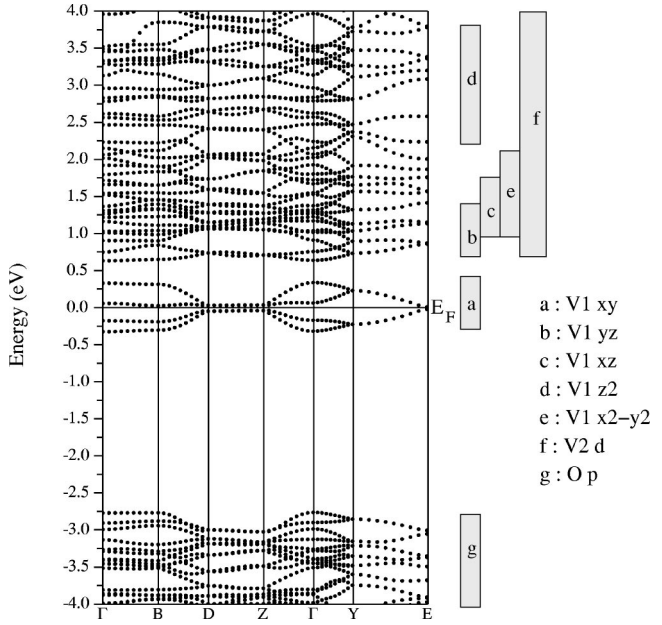

FIG. 2. DFT results for CsV_2O_5. The path is along $\Gamma=(0,0,0)$, $B=(-\pi,0,0)$, $D=(-\pi,0,\pi)$, $Z=(0,0,\pi)$, Γ, $Y=(0,\pi,0)$, and $E=(-\pi,\pi,\pi)$. Also shown as rectangles is the band character (in the local coordinate system) where V1=V^{4+} and V2=V^{5+}.

In Fig. 2 the energy bands for CsV_2O_5 along the path $\Gamma BDZ\Gamma YE$ are shown. Since the unit cell of CsV_2O_5 contains four formula units, i.e., four V^{4+} and four V^{5+}, there are four bands around the Fermi level which correspond to V^{4+} $3d$ orbitals. These bands are separated by an energy gap of about 2 eV from the lower O p valence bands and an energy gap of about 0.5 eV from the upper conduction bands. The conduction bands up to 4 eV are of V-3d nature. There are a few points to be noted here: (i) The energy range on the CsV_2O_5 bands is of the same order of magnitude as it is in α'-NaV_2O_5 (Ref. 17) and γ-LiV_2O_5 (Ref. 23). (ii) The contribution of V^{5+} $3d$ is mostly in the upper conduction bands, starting from about 0.75 eV above the Fermi level, and have a very small contribution at the Fermi level, indicating that, contrary to α'-NaV_2O_5 and γ-LiV_2O_5, here the system is close to complete charge ordering. (iii) There is no dispersion along the x axis while along the z axis (chain direction) the dispersion is non-negligible and of about 300 meV. Along the y axis the LDA bands show a small dispersion which corresponds to interchain interactions. In order to investigate the dimension-dependent behavior of CsV_2O_5, we show in Fig. 3(a) the partial density of states (DOS) of the V^{4+} $3d$ orbitals for CsV_2O_5. For comparison we have also plotted in Fig. 3(b) the partial density of states of V1 $3d$

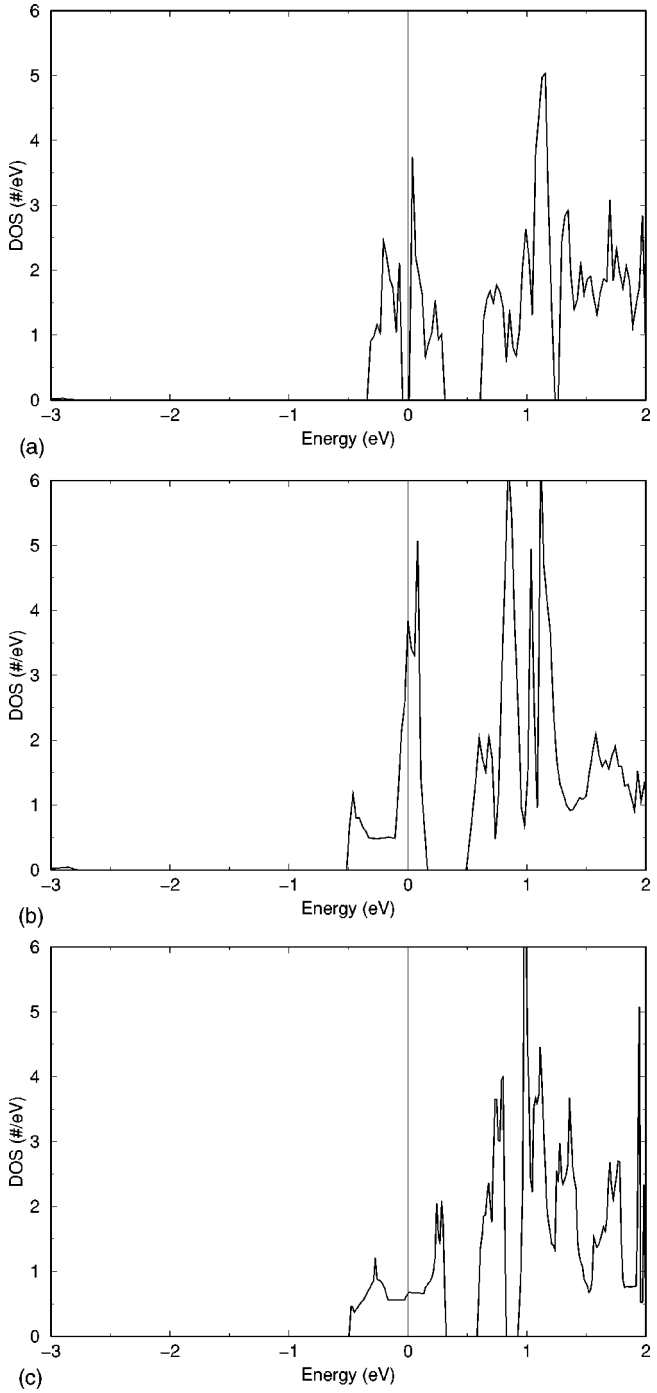

FIG. 3. Partial density of states of the V^{4+} $3d$ orbitals in (a) CsV_2O_5, (b) γ-LiV_2O_5, and (c) α'-NaV_2O_5 obtained from DFT. Compare the distinct behavior at band edges around the Fermi level.

orbitals for γ-LiV_2O_5 (Ref. 23) and in Fig. 3(c) that of V $3d$ orbitals for α'-NaV_2O_5. Note that, while the γ-LiV_2O_5 and α'-NaV_2O_5 DOS show the characteristic quasi-one-dimensional (quasi-1D) van Hove singularities near the band edges around the Fermi level, this is not the case for the Cs compound. The DOS for CsV_2O_5 shows more a 2D behavior than 1D. (iv) In the global frame of reference, the character of the bands around the Fermi level turn out to be that of d_{z^2} with small admixture from $d_{x^2-y^2}$ character. Rotation to a local coordinate system with the z axis aligned along the (*V-apical O*) direction for individual pyramids transforms this to d_{xy} character, in agreement with the crystal field analysis of a V^{4+} ion in the pyramidal environment.[14]

The band-structure analysis leads us to the conclusion that interdimer coupling is non-negligible. If the system would have been a pure dimer system, we would have expected no dispersion in any direction. The existence of a non-negligible dispersion tells us that a model of unlinked dimers is too simple and there must be some interdimer coupling to explain the band picture. From the DOS analysis we learn that interdimer interactions in both z and y directions are important for the electronic properties. The possible role of the $V^{5+}O_4$ tetrahedra in this context will be investigated in the next section.

IV. MICROSCOPIC MODEL (EFFECTIVE MODEL)

In order to understand the nature of the ground state in CsV_2O_5 we need to determine the appropriate microscopic model which explains the low-energy physics of this compound. We have therefore applied the so-called *downfolding method* offered by the new and generalized version of the LMTO (Ref. 31) method, together with a tight-binding (TB) analysis on the band-structure results. The downfolding technique consists of integrating out the high energy degrees of freedom so as to describe the details of LDA energy bands close to the Fermi energy in terms of few-orbital effective Hamiltonians. From this analysis, we can extract the effective hopping matrix elements t_{ij} between vanadium ions in CsV_2O_5 [by Fourier transform of the downfolded Hamiltonian $H(k) \rightarrow H(R)$] which reproduce the behavior of the LDA bands close to the Fermi level. Since as seen in the previous section the contribution of the V^{5+} $3d$ orbitals around the Fermi level is very small, and the biggest contribution comes from the V^{4+} $3d_{xy}$ orbital, a one-orbital effective tight-binding Hamiltonian should give a good description of the low-energy physics. The tight-binding Hamiltonian, therefore, can be written as

$$H_{TB} = -\sum_{\langle i,j \rangle} t_{ij}(c_j^\dagger c_i + c_i^\dagger c_j), \tag{1}$$

where i and j denote a pair of V^{4+} ions labeled each one by (n,s) where n denotes the unit cell and $s=1,2,3,4$ V^{4+} ions in the unit cell. In Fig. 4 all the considered hoppings t_1, t_2, t_3, and t_5 have been drawn. The subscripts 1, 2, 3, and 5 indicate, respectively, that the hopping integral is between first nearest neighbors (NN), second NN, third NN, and fifth NN. The hopping term t_4, which connects two V^{4+} ions belonging to two different layers along x, has been neglected due to its vanishingly small value. Note here that no hopping terms have been considered along the x direction, since as we have learned from the band picture, there is no dispersion along this direction and that means that the interlayer coupling along x must be negligible. In Fig. 5 we show a comparison of the *downfolding* TB bands to the LDA bands. We observe that not only is the hopping corresponding to the

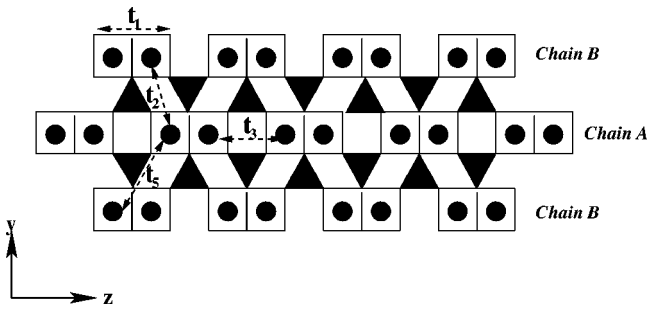

FIG. 4. Hopping parameters corresponding to the tight-binding modeling of CsV_2O_5. Not shown is the on-site energy ε_0 of the V^{4+} site. While t_1 corresponds to a direct V^{4+}-O-V^{4+} superexchange path, t_2, t_3, and t_5 are defined by paths through the neighboring V^{5+} O_4 tetrahedra.

intradimer interaction t_1 important but also the interdimer matrix element t_3 along z is considerable. A model with only t_1 and t_3, i.e., alternating chains, shows a dispersion relation of the form

$$E = \pm \sqrt{t_1^2 + t_3^2 + 2t_1 t_3 \cos k_z}, \tag{2}$$

which is symmetric with respect to $E=0$ (i.e., to E_F) and does not account for the band splittings in the paths Γ-D and Γ-Y. These features are described by the interchain hopping parameters along the y direction, t_2 and t_5, though they are much smaller than t_1 and t_3. Note that the TB results show an artificial band crossing along the paths B-D and Z-Γ. We have analyzed this result and seen that the inclusion of longer-ranged interactions lifts this artificial crossing.

Concerning the nature of the hopping integrals, we observe that the values of the dominant hopping parameter $t_1 = 0.12$ eV (which agrees with the overall bandwidth of the V^{4+}-d_{xy}-derived low-energy bands in CsV_2O_5) is smaller than the dominant hopping parameter for α'-NaV_2O_5,[17] $t_a = 0.37$ eV, and γ-LiV_2O_5,[23] $t_a = 0.35$ eV. This difference

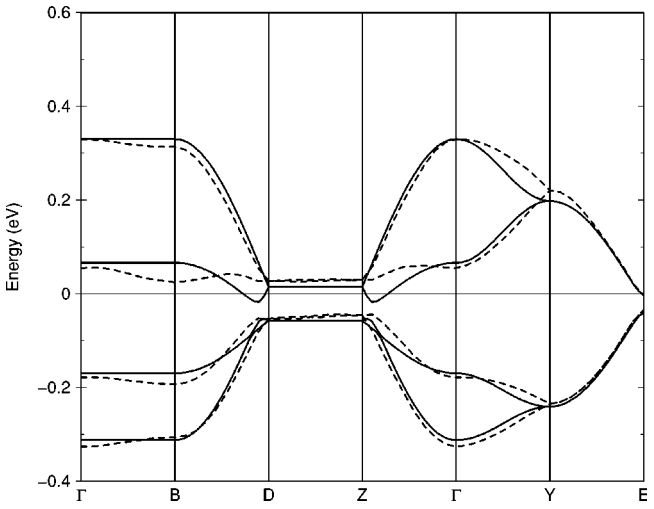

FIG. 5. Comparison of the tight-binding bands (solid lines) with the DFT bands (dashed lines). The tight-binding parameters (see Fig. 4) are (in eV) $\varepsilon_0 = -0.0215$, $t_1 = 0.117$, $t_2 = 0.015$, $t_3 = 0.097$, and $t_5 = 0.050$.

can be explained by the nature of the path. While t_1 in CsV_2O_5 corresponds to a *V-O-V* path in between two *edge*-sharing square pyramids, t_a in α'-NaV_2O_5 and γ-LiV_2O_5 corresponds to a *V-O-V* path between two *corner*-sharing square pyramids. This feature has important implications in the strength of the exchange interaction as has been pointed out in Ref. 14. Also note that the same kind of *edge*-sharing pyramids are also present in α'-NaV_2O_5 and γ-LiV_2O_5 (Ref. 23) with effective hopping values smaller than t_a and similar to t_1 in CsV_2O_5.

About the nature of the rest of the hopping integrals in CsV_2O_5, we observe that t_2, t_3, and t_5 correspond to V^{4+}-V^{4+} paths through the bridging V^{5+} O_4 tetrahedra with different lengths and angles. Beltrán-Porter *et al.*[32] studied, based on geometrical considerations, the various superexchange paths for the case of vanadyl phosphates. In particular they considered the VOPO compound. VOPO and CsV_2O_5 have a similar monoclinic structure if one identifies the P^{5+} O_4 tetrahedra and V^{4+} O_5 square pyramids in VOPO with the V^{5+} O_4 tetrahedra and $V^{4+}O_5$ square pyramids in CsV_2O_5, respectively. As argued by Beltrán-Porter *et al.*, based on the formation of coherent molecular electron orbitals, the coupling between two V^{4+} through bridging oxygens for separated pyramids is weaker than those via the pathways involving V^{5+} ions. Furthermore, double-bridging modes, involving two V^{5+} ions, as in t_2 and t_3 (see Fig. 4), can be stronger than single bridging modes involving one V^{5+} ion as in t_5. These interactions can be as strong as paths of the type t_1, i.e., V^{4+}-O-V^{4+}, where the square pyramids are linked to each other by sharing an edge. Geometrical considerations then lead to a relative order of importance among the various bridging modes, which for CsV_2O_5 is observed to be $t_3 > t_5 > t_2$. We note here that while in CsV_2O_5 we have seen that the dimers are formed by the edge-sharing pyramids (t_1) with the predominant interdimer interaction formed by the V^{4+}-V^{4+} interaction bridged by V^{5+} O_4 (t_3), in VOPO these roles are interchanged in the sense that dimers are formed by V^{4+} O_5 square pyramids bridged by P^{5+} O_4 groups[11,33] (t_3) and the interdimer interaction is formed by neighboring V^{4+} O_5 pyramids (t_1). This is due to the different type of distortion in the square pyramids as well as different angle and distance relations between these two compounds.

Using the relation $J_1 = 4t_1^2/U$, U being the on-site Coulomb electron-electron interaction, and considering $U \sim 2.8$ eV,[17] the DFT calculation gives an estimate of the intradimer exchange coupling, $J_1 \sim 225$ K.

To summarize, the conclusions that we draw from the above analysis is that *ab initio* calculations support an alternating chain behavior for CsV_2O_5 along z with weaker interchain interactions along y.

V. SUSCEPTIBILITY

In order to test the results obtained from the *ab initio* calculation we only have available two sets of susceptibility data[22,26] as a function of temperature which do not completely agree quantitatively with each other. We consider here the data by Isobe and Ueda.[22] These authors proposed

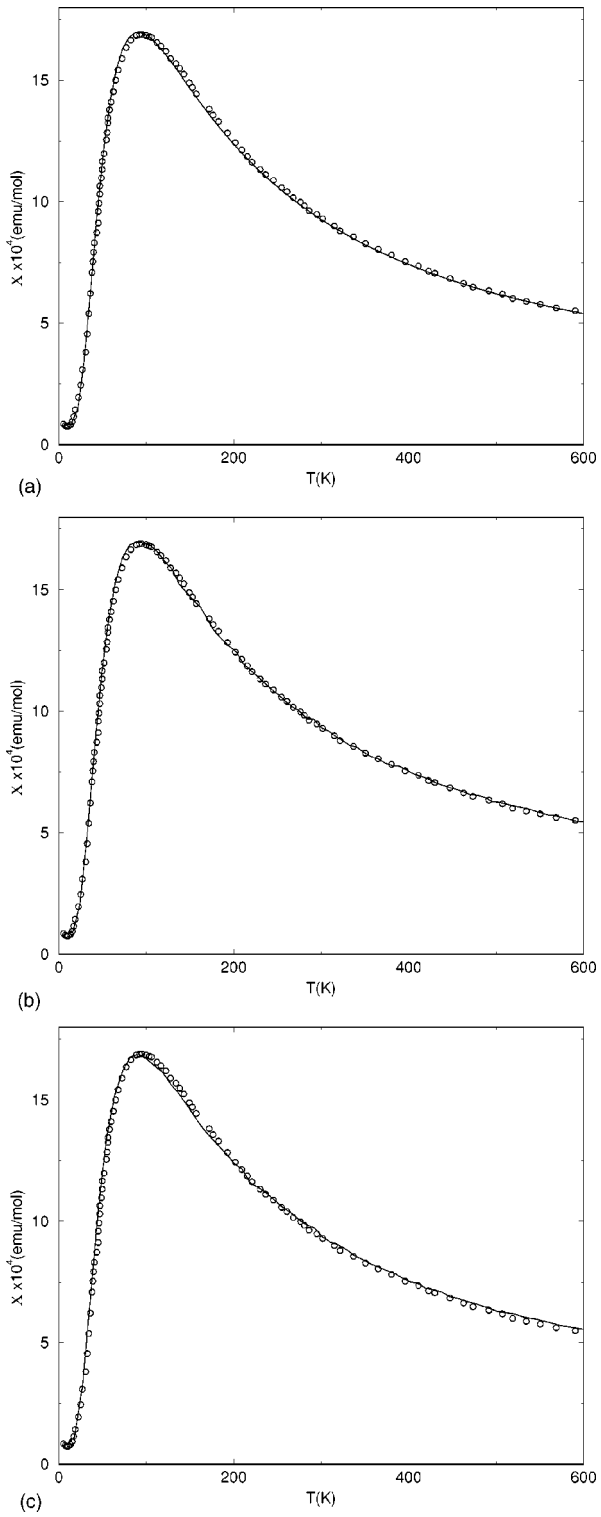

FIG. 6. Temperature dependence of the magnetic susceptibility of CsV_2O_5. The dots correspond to the experimental data by Isobe and Ueda (Ref. 22) where the Curie contribution has been subtracted. The solid lines show a fit to (a) spin-$\frac{1}{2}$ Heisenberg dimer with $J/k_B = 146$ K, $g = 1.77$, (b) spin-$\frac{1}{2}$ alternating Heisenberg chain with $\delta = 0.8$, $J_1/k_B = 146$ K, $g = 1.79$, and (c) spin-$\frac{1}{2}$ alternating Heisenberg chain with $\delta = 0.6$, $J_1/k_B = 146$ K, $g = 1.81$.

that their experimental data are well fitted by the susceptibility of a spin-$\frac{1}{2}$ dimer system with $H = J\mathbf{S}_1 \cdot \mathbf{S}_2$ given by

$$\chi_{raw} = \chi_{CsV_2O_5} + \chi_{imp} = \frac{Ng^2\mu_B^2}{k_B T} \frac{1}{3 + \exp(J/k_B T)} + \chi_0 + \chi_{imp}, \quad (3)$$

with a g factor of 1.8, $J = 146$ K, and $\chi_0 = 8 \times 10^{-5}$ emu/mol. We have reanalyzed the data by considering the temperature dependence of the susceptibility for a spin-$\frac{1}{2}$ alternating Heisenberg chain with

$$H = \sum_n (J_1 \mathbf{S}_{2n} \cdot \mathbf{S}_{2n+1} + J_2 \mathbf{S}_{2n+1} \cdot \mathbf{S}_{2n+2}), \quad (4)$$

with $J_1 > 0$ and $J_2 > 0$ (antiferromagnetic couplings) obtained by the stochastic quantum Monte Carlo method.[34] We define the parameter $\alpha = J_2/J_1$ which measures the ratio of the inter- and intradimer couplings. $\alpha = 0$ corresponds to the dimer model. We introduce also an additional parameter δ so that $J_1 = J(1+\delta)$, $J_2 = J(1-\delta)$ and therefore $\alpha = (1-\delta)/(1+\delta)$.

In Fig. 6(a) we show the comparison of the experimental data to the dimer-model susceptibility given by Eq. (3). We find, in fact, that the best fit corresponds to $J = 146$ K, $\chi_0 = 8 \times 10^{-5}$ emu/mol and a value of $g = 1.77$, somewhat smaller than the one proposed in Ref. 22. Figures 6(b) and 6(c) show the comparison of the experimental data to the spin-$\frac{1}{2}$ alternating Heisenberg chain model for $\delta = 0.8$ ($\alpha = 0.11$) and $\delta = 0.6$ ($\alpha = 0.25$), respectively. We observe that values of α up to 0.25 give still very good fits to the susceptibility data by choosing appropriate g and J parameters. This analysis makes plausible our *ab initio* results: namely, the fact that the interdimer interactions can be also significant.[35]

The important conclusion that we gain from this susceptibility analysis is that it is a very hard task to determine the behavior of a compound only from susceptibility fits. Extra information is needed so as to minimize the possible options. For instance, electron-spin-resonance (ESR) experiments could complement the susceptibility measurements by delivering the value of the gyromagnetic factor. There are in the literature other examples (e.g., VOPO) where the only examination of the susceptibility led to a wrong interpretation of the behavior of the system.[36]

VI. CONCLUSIONS

We have presented *ab initio* band-structure calculations for CsV_2O_5, a low-dimensional spin-gapped system and member of the alkali-vanadate family AV_2O_5 (A = Na, Li, Cs) which has a similar monoclinic structure as the most studied VOPO. By means of a *downfolding* tight-binding analysis, we observe that the behavior of this system can be best described by a spin-$\frac{1}{2}$ alternating chain model with weak interchain interactions. This proposal has been complemented by an analysis of available susceptibility data for this compound. A reexamination of the temperature dependence of the experimental susceptibility leads us to the conclusion

that an alternating chain model can also provide a good fitting by choosing appropriate g and J values. We have discussed the structural, electronic, and magnetic similarities and differences between CsV_2O_5, α'-NaV_2O_5, and γ-LiV_2O_5, VOPO.

With this work we would like to draw attention to this compound which shows interesting features, especially since it has a lot of points of comparison to the most studied VOPO. We think that new experimental studies like ESR, inelastic scattering, Raman scattering, and the study of a possible field-induced magnetic ordering under a very strong magnetic field would be helpful to unveil the behavior of this material.

ACKNOWLEDGMENT

One of us (R.V.) thanks the German Research Foundation (DFG) for financial support.

[1] F.D.M. Haldane, Phys. Rev. Lett. **50**, 1153 (1983).
[2] See E. Dagotto and T.M. Rice, Science **271**, 618 (1996).
[3] J.C. Bonner and M.E. Fisher, Phys. Rev. **135**, A640 (1964); J.C. Bonner and H.W.J. Blöte, Phys. Rev. B **25**, 6959 (1982).
[4] J. Darriet and L.P. Regnault, Solid State Commun. **86**, 409 (1993).
[5] R.S. Eccleston, M. Uehara, J. Akimitzu, H. Eisaki, N. Motoyama, and S. Uchida, Phys. Rev. Lett. **81**, 1702 (1998).
[6] M. Azuma, Z. Hiroi, M. Takano, K. Ishida, and Y. Kitaoka, Phys. Rev. Lett. **73**, 3463 (1994).
[7] T. Kato, K. Takatsu, H. Tanaka, W. Shiramura, M. Mori, K. Nakajima, and K. Kakurai, J. Phys. Soc. Jpn. **67**, 752 (1998).
[8] See A. Oosawa, T. Kato, H. Tanaka, K. Kakurai, M. Müller, and H.-J. Mikeska, Phys. Rev. B **65**, 094426 (2002) and references therein.
[9] G. Xu, C. Broholm, D.H. Reich, and M.A. Adams, Phys. Rev. Lett. **84**, 4465 (2000).
[10] M. Hase, I. Terasaki, and K. Uchinokura, Phys. Rev. Lett. **70**, 3651 (1993).
[11] A.W. Garrett, S.E. Nagler, D.A. Tennant, B.C. Sales, and T. Barnes, Phys. Rev. Lett. **79**, 745 (1997); G.S. Uhrig and B. Normand, Phys. Rev. B **63**, 134418 (2001).
[12] H. Kageyama *et al.*, Phys. Rev. Lett. **82**, 3168 (1999).
[13] P. Lemmens, K.-Y. Choi, E.E. Kaul, Ch. Geibel, K. Becker, W. Brenig, R. Valentí, C. Gros, M. Johnsson, P. Millet, and F. Mila, Phys. Rev. Lett. **87**, 227201 (2001).
[14] Y. Ueda, Chem. Mater. **10**, 2653 (1998).
[15] M. Onoda and N. Nishiguchi, J. Solid State Chem. **127**, 359 (1996); H. Iwase *et al.*, J. Phys. Soc. Jpn. **65**, 2397 (1996).
[16] See, for instance, M. Onoda and A. Ohyama, J. Phys.: Condens. Matter **10**, 1229 (1998); P. Millet *et al.*, Phys. Rev. B **57**, 5005 (1998).
[17] H. Smolinski, C. Gros, W. Weber, U. Peuchert, G. Roth, M. Weiden and C. Geibel, Phys. Rev. Lett. **80**, 5164 (1998).
[18] P. Horsch and F. Mack, Eur. Phys. J. B **5**, 367 (1998).
[19] T. Ohama, H. Yasuoka, M. Isobe, and Y. Ueda, Phys. Rev. B **59**, 3299 (1999).
[20] See, for instance, J. Lüdecke, A. Jobst, S. van Smaalen, E. Morre, C. Geibel and H.-G. Krane, Phys. Rev. Lett. **82**, 3633 (1999); J.L. de Boer, A.M. Meetsma, J. Baas and T.T.M. Palstra, *ibid.* **84**, 3962 (2000).
[21] M. Isobe and Y. Ueda, J. Phys. Soc. Jpn. **65**, 1178 (1996).
[22] M. Isobe and Y. Ueda, J. Phys. Soc. Jpn. **65**, 3142 (1996).
[23] R. Valentí, T. Saha-Dasgupta, J.V. Alvarez, K. Pozgajcic, and C. Gros, Phys. Rev. Lett. **86**, 5381 (2001).
[24] Y. Takeo *et al.*, J. Phys. Chem. Solids **60**, 1145 (1999).
[25] A. Hübsch, C. Waidacher, and K.W. Becker, Phys. Rev. B **64**, 241103 (2001).
[26] J. Mur and J. Darriet, C. R. Acad. Sci., Ser. II: Mec., Phys., Chim., Sci. Terre Univers, **300**, 599 (1985).
[27] K. Waltersson and B. Forslund, Acta Crystallogr., Sect. B: Struct. Crystallogr. Cryst. Chem. **33**, 789 (1977).
[28] P. Blaha, K. Schwarz, and J. Luitz, computer code WIEN97, A Full Potential Linearized Augmented Plane Wave Package for Calculating Crystal Properties, Karlheinz Schwarz, Technical University Wien, Vienna, 1999) [updated version of P. Blaha, K. Schwarz, P. Sorantin, and S.B. Trickey, Comput. Phys. Commun. **59**, 399 (1990)].
[29] O.K. Andersen, Phys. Rev. B **12**, 3060 (1975).
[30] J.P. Perdew, S. Burke, and M. Ernzerhof, Phys. Rev. Lett. **77**, 3865 (1996).
[31] O.K. Andersen and T. Saha-Dasgupta, Phys. Rev. B **62**, R16219 (2000) and references there in.
[32] D. Beltrán-Porter, P. Amorós, R. Ibáñez, E. Martínez, and A. Beltrán-Porter, Solid State Ionics **32/33**, 57 (1989).
[33] T. Saha-Dasgupta *et al.* (unpublished).
[34] Data provided by C. Gros.
[35] A fit of susceptibility data to a model with interchain couplings has not been considered here.
[36] D.C. Johnston, J.W. Johnston, D.P. Goshorn, and A.J. Jacobson, Phys. Rev. B **35**, 219 (1987).